Recombination dynamics of clusters in intense extreme-ultraviolet and near-infrared fields

PAPER

CrossMark

Recombination dynamics of clusters in intense extreme-ultraviolet and near-infrared fields

Bernd Schütte[1,2], Tim Oelze[3], Maria Krikunova[3], Mathias Arbeiter[4], Thomas Fennel[4], Marc J J Vrakking[1] and Arnaud Rouzée[1]

1   Max-Born-Institut, Max-Born-Str. 2 A, D-12489 Berlin, Germany
2   Department of Physics, Imperial College London, South Kensington Campus, SW7 2AZ London, UK
3   Institut für Optik und Atomare Physik, Technische Universität Berlin, Eugene-Wigner-Bldg EW 3-1, Hardenbergstr. 36, D-10623 Berlin, Germany
4   Institute of Physics, University of Rostock, Universitätsplatz 3, D-18055 Rostock, Germany

E-mail: schuette@mbi-berlin.de

Abstract

We investigate electron-ion recombination processes in clusters exposed to intense extreme-ultraviolet (XUV) or near-infrared (NIR) pulses. Using the technique of reionization of excited atoms from recombination (REAR), recently introduced in Schütte *et al* (2014 *Phys. Rev. Lett.* **112** 253401), a large population of excited atoms, which are formed in the nanoplasma during cluster expansion, is identified under both ionization conditions. For intense XUV ionization of clusters, we find that the significance of recombination increases for increasing cluster sizes. In addition, larger fragments are strongly affected by recombination as well, as shown for the case of dimers. We demonstrate that for mixed Ar–Xe clusters exposed to intense NIR pulses, excited atoms and ions are preferentially formed in the Xe core. As a result of electron-ion recombination, higher charge states of Xe are efficiently suppressed, leading to an overall reduced expansion speed of the cluster core in comparison to the shell.

1. Introduction

The ionization processes in rare-gas clusters interacting with intense light pulses exhibit significant differences depending on the laser wavelengths. In the near-infrared (NIR) regime, multiphoton and optical field ionization trigger the charging of the cluster [1, 2]. Subsequently, enhanced ionization via cooperative effects and resonance heating play an important role in further charging the cluster. The internal field, which can be suppressed via screening of the laser field or greatly enhanced near the plasmon resonance, heats the electrons trapped within the cluster such that electron impact ionization becomes very efficient as a consequence of avalanche effects. A comparison between atoms and clusters interacting with the same light pulses at a wavelength of 1064 nm revealed that the observed ionic charge states were significantly higher in the case of clusters as a result of efficient heating [3]. In contrast, when a cluster is exposed to intense extreme-ultraviolet (XUV) light pulses with photon energies above the atomic ionization potential, the predominant excitation process is single-photon ionization of atoms in the cluster. At the rising edge of the XUV light pulse, electrons are thus directly emitted from the cluster. Subsequently emitted electrons experience a kinetic energy downshift due to the growing cluster potential. In the photoelectron spectrum, this leads to the observation of a characteristic multistep plateau [4]. The Coulomb barrier becomes larger by further ionization processes, and as a result, electrons get trapped in the cluster and a nanoplasma is formed. Collisional and resonance heating are suppressed in the XUV range such that ionization heating [5], i.e. the electron excess energy from vertical photoionization, becomes the main nanoplasma heating mechanism. In contrast to the NIR case, the number of ions with higher charge states is typically reduced in clusters with respect to atoms [6, 7].

Despite the differences in the ionization processes of clusters under NIR and XUV ionization, many similarities in the cluster expansion and dissociation dynamics were observed. In both cases, a substantial part of the electrons remain trapped within the cluster, since their kinetic energies are insufficient to overcome the cluster Coulomb barrier. As these electrons are not bound to a specific atom anymore, they can freely move inside the cluster, and together with the ions they form a nanoplasma, where collisional energy exchange takes place. A fraction of the electrons gain sufficient energy to leave the cluster by evaporation, leading to a characteristic thermal electron distribution in the electron kinetic energy spectrum that was observed both in the NIR range [8] as well as in the vacuum-ultraviolet [9] and XUV regimes [10]. A substantial fraction of the quasifree electrons eventually recombines with ions in the expanding cluster [1, 11–16].

In a recent study, we reported on the observation of very slow electrons that resulted from electron-ion recombination to highly excited Rydberg states following the ionization of atomic clusters by intense XUV pulses and the subsequent reionization by the dc detector electric field [7], a process that is known as frustrated recombination [12]. In a second investigation, electron-ion recombination in pure Ar and mixed Ar–Xe clusters upon ionization with intense XUV pulses was investigated using pump-probe spectroscopy. A weak NIR probe pulse was used for the reionization of excited atoms (REAR = Reionization of Excited Atoms from Recombination) [17]. A significant formation of excited atoms was observed, and the extracted time scale for recombination in mixed Ar–Xe clusters was found to be around 10 ps.

The understanding of electron-ion recombination processes can be improved by studying clusters formed of different species and sizes, and by using light pulses at various wavelengths. It is of particular interest to investigate how the fundamentally different ionization mechanisms of NIR pulses interacting with clusters influence the following nanoplasma dynamics.

In the current paper, we present a significantly extended time-resolved investigation of clusters ionized by intense XUV or NIR pulses, focusing our studies on the formation of excited atoms and ions by charge recombination. After a description of the experimental setup in section 2, we present new results of electron-ion recombination in clusters ionized by intense XUV pulses from a high-order harmonic generation (HHG) source in section 3. In section 3.1, we show a study of recombination obtained after XUV ionization of Kr clusters, where similar features are observed as in the case of Ar and Ar–Xe clusters [17], thus demonstrating the general applicability of this approach. In section 3.2, we demonstrate that recombination becomes more efficient for increasing cluster sizes. In addition, we find that recombination and the formation of excited atoms are important for larger cluster fragments as well, as shown for dimers. Section 4 presents a first time-resolved investigation of charge recombination processes occurring in clusters ionized by intense NIR pulses in mixed Ar–Xe clusters. Our studies reveal that charge recombination preferentially takes place in the Xe core of the clusters, similar to the results on clusters ionized by intense XUV pulses. A summary is given in section 5.

2. Experimental setup

The Ti:sapphire laser system used for the experiments delivers (32 ± 2) fs pulses at a central wavelength of 790 nm, a repetition rate of 50 Hz and a maximum pulse energy of 35 mJ [18]. Intense XUV pulses are obtained by HHG, where the laser beam is focused into a 15 cm long gas cell by a spherical mirror with a focal length of 5 m. As generation medium, Ar is used at a static pressure of 7 mbar. After a propagation distance of 5 m, a 200 nm thick Al filter blocks the NIR light and all harmonics below the 11th order. The HHG radiation can be analyzed by an XUV spectrometer or directly be sent to the experimental station, where it is focused by a spherical AlMg/SiC multilayer mirror with a focal length of 75 mm in the center of a velocity map imaging (VMI) spectrometer. The mirror is designed for a peak reflectivity at 33 eV, but it also shows non-negligible reflection at lower photon energies. A typical XUV pulse duration was measured as (20 ± 3) fs via terahertz streaking [19, 20]. We note that this value can vary from day to day for different HHG settings. Most importantly, the shot-to-shot fluctuations are expected to be low. The XUV beam is focused to an estimated spot size of 3 μm, leading to an intensity of 2×10^{12} W cm^{-2}. This value is supported by the good agreement obtained with photoelectron spectra that are simulated for XUV-only ionization of the clusters [7]. We estimate an uncertainty of a factor of 2 for the absolute intensity, and 8% standard deviation for the shot-to-shot fluctuations mainly due to variations of the XUV pulse energy. In the interaction zone, the XUV beam interacts with a cluster beam obtained by a piezoelectric valve with a 0.5 mm diameter nozzle, from which the central part is selected by a 0.5 mm molecular beam skimmer. The cluster size is varied by changing the backing pressure and estimated according to the Hagena scaling law [21]. For the generation of mixed Ar–Xe clusters, a gas mixture containing 98% Ar atoms and 2% Xe atoms is expanded, which was previously shown to form clusters with a Xe core and an Ar shell [22, 23]. In this case, the cluster composition is estimated according to the sizes of pure Xe and Ar clusters that are formed at the given backing pressure, which are then multiplied by the ratios of the atoms in the gas mixture and summed up.

In the XUV–NIR pump-probe experiments, a small portion (10%) of the NIR pulse is split off before the harmonic generation using a beamsplitter. These NIR pulses can be time-delayed with respect to the XUV pulses. They are recombined with the XUV beam by a mirror with a hole that reflects the outer part of the NIR probe beam, while the XUV beam has a smaller beam diameter and passes through the hole. In the following, both beams propagate collinearly and are focused into the interaction zone by the same multilayer mirror. For the NIR cluster ionization experiments, the Al filter is moved out of the beam path, and no gas is used in the harmonic cell. The energies of both pump and probe NIR pulses are controlled by means of neutral density filters. We estimate an uncertainty for the absolute NIR intensities of 50%, and 4% standard deviation for the shot-to-shot fluctuations. For the NIR probe pulse, a typical intensity around 1×10^{13} W cm^{-2} is used, adjusted such that no ion or electron signal is observed from clusters with the probe pulse only.

Angle-resolved photoion and -electron spectra following the interaction of the cluster beam with the laser pulses are recorded by a VMI spectrometer [24]. An electric field up to 2 kV cm^{-1} accelerates the generated ions or electrons towards a multichannel plate / phosphor screen assembly. The two-dimensional momentum distributions are recorded by a CCD camera, from which we obtain the kinetic energy distributions by applying a standard Abel inversion procedure [25].

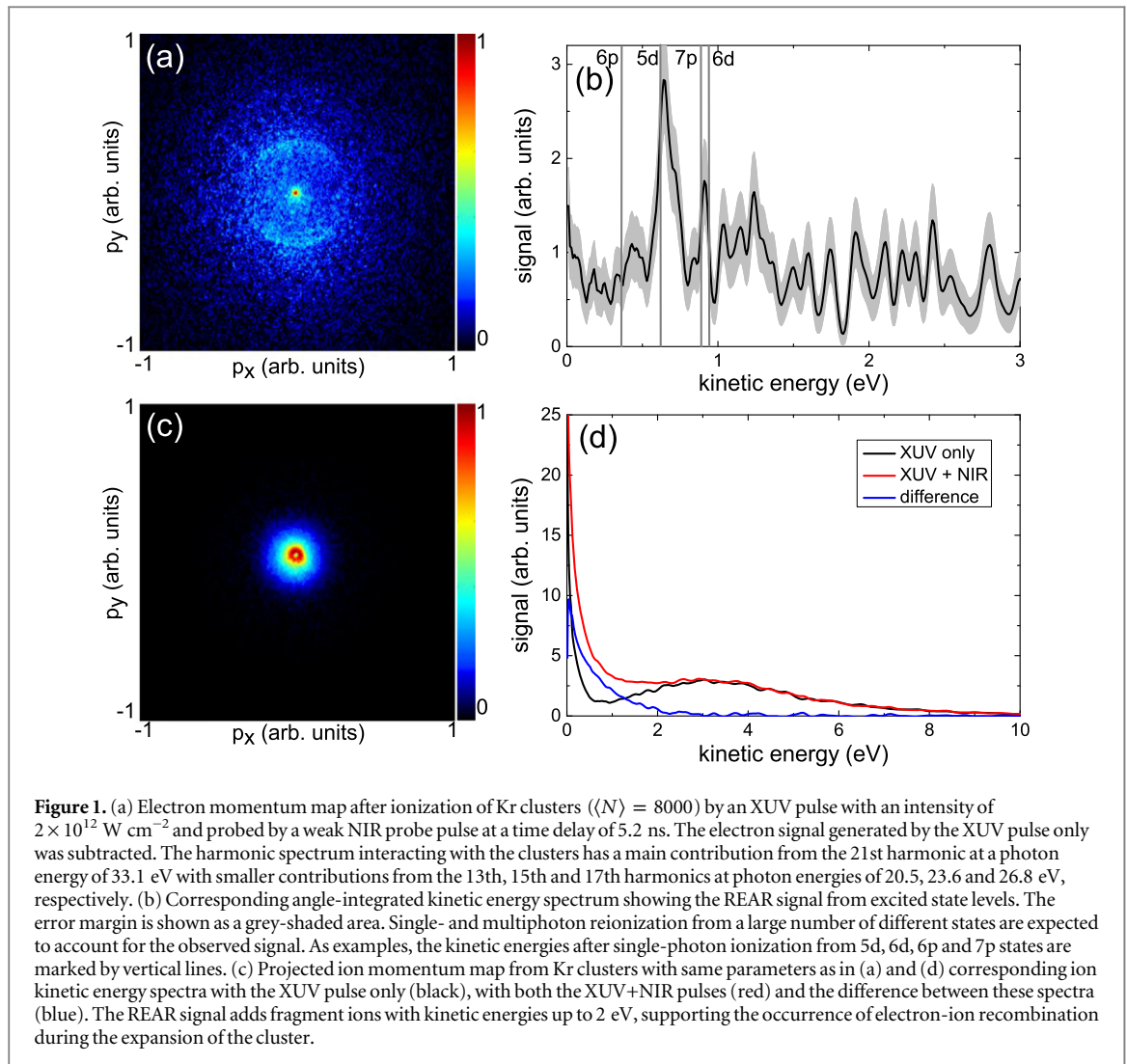## 3. Electron-ion recombination following intense XUV ionization of clusters

3.1. Spectral signatures of recombination in Kr clusters

Ionization of rare-gas clusters with intense XUV pulses leads to the formation of excited atoms in low- and high-lying Rydberg states due to an efficient charge recombination process that occurs when quasifree electrons are trapped within the cluster [7, 17]. The excited atoms can be observed by reionizing them using a weak probe pulse. This is shown in figure 1 for the case of Kr clusters, where reionization of the excited atoms by the NIR probe pulse leads to a ring structure in the electron momentum distribution, similar to the previous observation in Ar clusters [17]. Since the electron momentum distribution shown in figure 1(a) was taken at a delay of 5.2 ns between the XUV and NIR pulses, the effect of the cluster potential on the final kinetic energies of emitted electrons is negligible. Therefore, the observed distinct peaks in the kinetic energy spectrum in figure 1(b) are attributed to the reionization of different excited atomic states. Due to the high density of excited states in Kr and possible contributions from multiphoton ionization, a definite assignment of the measured peaks to specific states is challenging. As an example, the vertical lines in figure 1(b) show the expected kinetic energies of electrons after ionization by single NIR photons from the 5d, 6d, 6p and 7p singly-excited states of Kr.

In addition to recombination, two other mechanisms can possibly lead to the population of excited states, namely direct laser excitation and electron impact excitation by quasifree electrons. Direct laser excitation of neutral atoms can be excluded here, since the photon energies transmitted by the Al filter are well above the ionization threshold of Kr. Furthermore, in our recent study we demonstrated that by choosing low XUV photon energies it is also possible to exclude electron impact excitation as the main process for the formation of excited atoms [17], since the initial photoelectron energy can easily be chosen to be lower than the minimum energy required for the excitation of ground states atoms. While some of the electrons can gain additional energy by collisions, the majority of electrons are expected to undergo rapid expansion cooling in the expanding cluster. Therefore, the formation of a large number of excited atoms cannot be explained by electron impact excitation. Instead, the ion momentum map (figure 1(c)) and the kinetic energy spectra (figure 1(c)) provide further support for the idea of electron-ion recombination being responsible for the generation of excited atoms. Reionization by the weak NIR probe pulse leads to the detection of ions with kinetic energies up to 2 eV. Given that these ions are formed at a time at which the cluster has disintegrated completely (when no subsequent acceleration will take place), the neutral atoms ionized by the NIR laser must have acquired kinetic energy as transient ionic charge states at the beginning of the cluster expansion before being neutralized by electron-ion recombination. The existence of transient charge states was recently also demonstrated by fluorescence spectroscopy [26].

3.2. Recombination for different cluster sizes and cluster fragments

We further study recombination for different cluster sizes and cluster fragments. Experiments were performed in Ar clusters ionized by a strong XUV pulse and probed by a weak NIR pulse. In figure 2(a), we present the momentum map of Ar$^+$ ions, where the difference between spectra obtained by the XUV+NIR pulses and by the XUV pulse only is shown, at a time delay of 217 ps between the pulses. The strong signal at low momenta is attributed to REAR processes. In figure 2(b), angle-integrated kinetic energy spectra are depicted for the XUV pulse only and for XUV+NIR pulses at different time delays. At 1.3 and 7 ps, a large increase of the Ar$^+$ signal at higher kinetic energy is observed compared to the situation when using the XUV pulse only, which is attributed

Figure 1. (a) Electron momentum map after ionization of Kr clusters ($\langle N \rangle = 8000$) by an XUV pulse with an intensity of 2×10^{12} W cm^{-2} and probed by a weak NIR probe pulse at a time delay of 5.2 ns. The electron signal generated by the XUV pulse only was subtracted. The harmonic spectrum interacting with the clusters has a main contribution from the 21st harmonic at a photon energy of 33.1 eV with smaller contributions from the 13th, 15th and 17th harmonics at photon energies of 20.5, 23.6 and 26.8 eV, respectively. (b) Corresponding angle-integrated kinetic energy spectrum showing the REAR signal from excited state levels. The error margin is shown as a grey-shaded area. Single- and multiphoton reionization from a large number of different states are expected to account for the observed signal. As examples, the kinetic energies after single-photon ionization from 5d, 6d, 6p and 7p states are marked by vertical lines. (c) Projected ion momentum map from Kr clusters with same parameters as in (a) and (d) corresponding ion kinetic energy spectra with the XUV pulse only (black), with both the XUV+NIR pulses (red) and the difference between these spectra (blue). The REAR signal adds fragment ions with kinetic energies up to 2 eV, supporting the occurrence of electron-ion recombination during the expansion of the cluster.

to an efficient absorption of NIR energy at the plasmon resonance [27, 28]. At larger time delays of 83 ps and 217 ps, the low-energy peak is due to REAR.

We now compare the observed recombination signal for different cluster sizes. For an average cluster size of $\langle N \rangle = 18000$ atoms used here, the increase in the Ar$^+$ ion signal due to REAR in comparison to the signal obtained by the XUV pulse only is 95% at a time delay of 217 ps. In comparison, for a cluster size of $\langle N \rangle = 3500$ atoms, as used in [17] under similar conditions and at an XUV–NIR time delay of 200 ps, the signal enhancement by REAR is only 73%. This difference indicates a more efficient nanoplasma formation in larger clusters. We can estimate the critical cluster charge state q_{full}, where the direct photoemission is frustrated by [29]: $q_{full} = (\hbar\omega - I_P) r_S N^{1/3} / 14.4$ eVÅ. Here $\hbar\omega$ is the photon energy (33.1 eV), I_P is the atomic ionization potential (15.76 eV for Ar), r_S is the Wigner–Seitz radius (2.21 Å for Ar), and N is the cluster size. For an Ar$_{18000}$ cluster, direct photoemission is frustrated when 0.4% of all atoms (i.e. 70 atoms) in the cluster are ionized. In comparison, for an Ar$_{3500}$ cluster, only 40 atoms need to be ionized to fully frustrate direct photoemission, which, however, corresponds to a significantly larger fraction of 1.1% of all atoms in the cluster. The number N_{PA} of photo-activated electrons in a cluster is estimated according to $N_{PA} = NI_0\tau\sigma/\hbar\omega$. I_0 is the laser intensity (2×10^{12} W cm^{-2}), τ is the pulse duration (20 fs), and σ is the photoionization cross section (13.8 Mb at 33 eV [30]). For an Ar$_{18000}$ cluster we estimate $N_{PA} = 1870$, showing that 96% of the photo-activated electrons remain trapped in the cluster. In comparison, for an Ar$_{3500}$ cluster, 360 electrons are photoactivated, and 89% of these electrons remain trapped. The more efficient nanoplasma formation in the first case supports the observation of more efficient recombination in larger clusters. We note that focal volume averaging and the cluster size distribution in the experiment have an influence on the estimated numbers, but this will not affect the general trend of an increasing importance of nanoplasma formation in larger clusters.

In the following, we investigate the effects of recombination in larger fragments. A differential momentum map of Ar$_2^+$ dimers taken at a time delay of 217 ps between the XUV and NIR pulses is presented in figure 2(c).

Figure 2. (a) Ar^+ ion momentum map from Ar clusters with an average size of $\langle N \rangle = 18000$ after ionization by XUV pulses at an intensity of 2×10^{12} W cm^{-2} with a main HHG peak at 33.1 eV. The distribution represents the difference between an XUV+NIR measurement at a time delay of 217 ps and the signal obtained by the XUV pulse only. (b) Angle-integrated kinetic energy spectra obtained by the XUV pulse and by XUV+NIR pulses at different pump-probe time delays. (c), (d) same as in (a), (b) for Ar_2^+ ions.

The corresponding angle-integrated kinetic energy spectra in figure 2(d) recorded at different time delays reveal several effects induced by the probe pulse. At a short time delay of 1.3 ps, the plasmon resonance heating [27, 28] leads to additional laser energy absorption by the cluster resulting in an Ar_2^+ kinetic energy distribution that is slightly upshifted compared to the case where only the XUV pulse is present. This is similar to the observation in monomers, although the effect is significantly smaller for dimers. At delays of 83 and 217 ps, a strong peak appears in the spectrum below 1 eV that in analogy to the case of monomers (figure 2(b)) is attributed to reionization of excited dimers following electron-ion recombination processes. The kinetic energies of excited dimers are substantially smaller compared to singly-charged dimers that are present without the probe pulse, since the former are neutral throughout most of the cluster expansion time. We note that in contrast to monomers, the signal between 2 and 8 eV is slightly decreased for larger time delays, which is attributed to dissociation of the dimers induced by the probe pulse. Dissociation of dimers may also play a role at time delays of 1.3 and 7 ps. However, the cluster dynamics are strongly influenced by the resonant absorption of NIR laser energy at these time delays. It is therefore difficult to separate a contribution that can clearly be attributed to the dissociation of dimers.

4. Time-resolved investigation of recombination in clusters ionized by intense NIR pulses

Extensive formation of excited atoms was observed in clusters after ionization at different wavelengths, including the NIR regime [17]. Since nanoplasma formation with a large number of ions and quasifree electrons takes place under these conditions, electron-ion recombination is expected to play an important role here as well. In contrast to the XUV case, however, direct laser excitation and electron impact excitation may also be significant. Similar to the experiments with intense XUV pulses reported in [17], mixed Ar-shell Xe-core clusters were used to distinguish between effects from different layers of the clusters. While this gives us an experimental approach to study effects in the inner core and in the outer shell of clusters, we note that the dynamics can also be influenced by the different masses of the atomic species. In figure 3, Xe^+ ion kinetic energy spectra are shown at different delays between the NIR pump and probe pulses. At the early stage of the cluster expansion around 1 ps, the Xe^+ signal above 10 eV increases significantly. This signal was previously attributed to an enhanced cluster explosion due to strong heating and ionization when the frequency of the probe laser matches the plasmon frequency of the expanding cluster [27, 28]. In the Xe core, this effect was strongly suppressed following
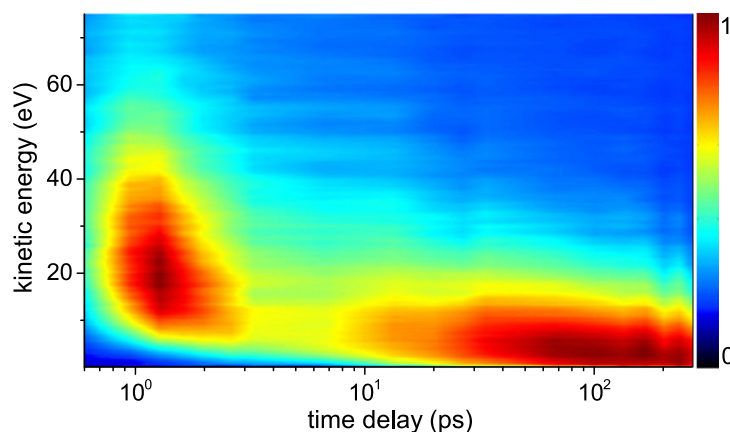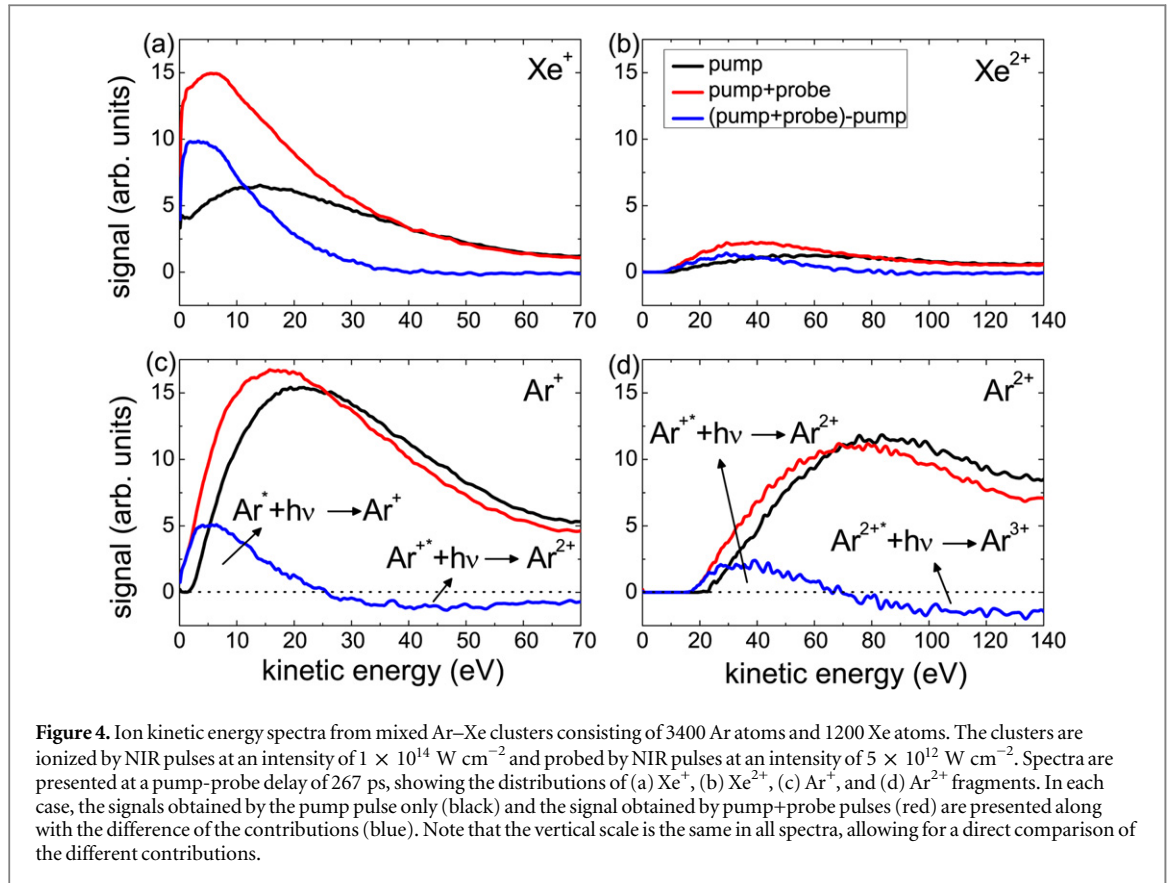
Figure 3. Time-resolved Xe$^+$ ion kinetic energy spectra after NIR ionization of mixed Ar–Xe clusters with an average composition of 3400 Ar atoms in the shell and 1200 Xe atoms in the core. The spectra represent the difference between spectra obtained in an NIR-pump+NIR-probe experiment and in an NIR-pump-pulse-only experiment, and were recorded at different time delays between the two pulses. The intensities of the pump and probe pulses are 1×10^{14} and 5×10^{12} W cm^{-2}, respectively. Note that the time axis is plotted logarithmically in order to be able to show the different processes occurring on time scales from a few hundred fs to a few hundred ps. The kinetic energy spectra are smoothed by a running average over 10 bins in energy, where each bin has a width of 0.2 eV. Here similar results are obtained compared to a previous experiment using XUV pump and NIR probe pulses in [17].

ionization with an intense XUV pulse [17]. The larger Xe$^+$ signal in the current case demonstrates the fundamentally different response for the cluster ionization and expansion when using NIR pump pulses, where a higher degree of ionization is achieved, leading to a large remaining population of free electrons even in the presence of significant recombination. However, in spite of the distinct differences upon XUV and NIR ionization of clusters, qualitatively similar effects are observed after the pump light pulse has ended. At time delays above 10 ps, the kinetic energy spectra in figure 3 are dominated by contributions at lower kinetic energies, as previously observed in the case of XUV ionization of clusters (figure 1(d)). The signal at low kinetic energies is also present for longer time delays and represents the formation of excited atoms during the cluster expansion. Remarkably, the ions generated by the probe pulse have kinetic energies reaching up to 35 eV (see also kinetic energy spectra of Xe$^+$ ions with and without probe pulse in figure 4(a)). The observation of excited atoms with such high kinetic energies strongly suggests that they originate from reionization processes by the NIR probe pulse upon electron-ion recombination processes, as in the XUV case. After initial ionization by the pump pulse, ions gain recoil energy up to the point where they recombine with quasifree electrons. Next, the excited atoms propagate with almost constant velocity as neutral particles up to their reionization by the probe pulse. Note that neutral atoms with kinetic energies up to 1 MeV (i.e. almost as high as the ion kinetic energies) were observed after NIR irradiation of clusters in [31]. In that study, two orders of magnitude higher intensities and particularly high cluster densities exceeding 10^{12} clusters cm^{-3} were used, which is more than 100 times larger compared to the present study. In [31], electron transfer from Rydberg excited neighboring clusters was discussed as one of the main neutralization mechanism that allows the ions to gain a large kinetic energy before they recombine with electrons. In contrast, electrons and ions that undergo recombination in the present study, originate from the same cluster, a process that takes place within the first few ps after cluster ionization.

Time-resolved experiments allow us to determine the final kinetic energies of charged and neutral cluster fragments. Between 10 and 100 ps, the kinetic energies of Xe$^+$ ions decrease for increasing time delays (figure 3). This is because ions can gain additional energy after the REAR process due to repulsive forces between the ions, and the amount of kinetic energy gain depends on the expansion of the cluster at the time of reionization. However, as the average distance between atoms in the expanding cluster decreases for larger delays above 100 ps, this kinetic energy gain becomes negligible, and we can assume that the individual fragments do not interact anymore with each other at a time delay of 267 ps. By measuring the kinetic energies of the excited atoms using the weak NIR probe pulse (difference spectra in figure 4), we obtain a good approximation for the final kinetic energies of the neutral fragments, and we can compare these to the final kinetic energies of the singly-charged fragments obtained with the pump pulse only. In figure 4(a), the kinetic energy distribution resulting from the reionization of excited Xe atoms (blue difference curve) has a maximum at 3.5 eV, whereas the kinetic energy distribution of Xe$^+$ ions measured with the NIR pump pulse only is peaked at 15 eV. In the case of Ar, the kinetic energy distribution has a maximum at 5 eV for the neutral atoms and at 22 eV for the singly-charged ions obtained by the pump pulse (figure 4(c)). These results demonstrate that ions undergoing recombination acquire a much lower kinetic energy compared to ions that do not recombine. The large differences can be explained by a combination of two effects: ions in the nanoplasma are expected to expand more slowly by hydrodynamic forces, in contrast to a faster Coulomb explosion of ions whose charges are not shielded by

Figure 4. Ion kinetic energy spectra from mixed Ar–Xe clusters consisting of 3400 Ar atoms and 1200 Xe atoms. The clusters are ionized by NIR pulses at an intensity of 1×10^{14} W cm^{-2} and probed by NIR pulses at an intensity of 5×10^{12} W cm^{-2}. Spectra are presented at a pump-probe delay of 267 ps, showing the distributions of (a) Xe$^+$, (b) Xe^{2+}, (c) Ar$^+$, and (d) Ar^{2+} fragments. In each case, the signals obtained by the pump pulse only (black) and the signal obtained by pump+probe pulses (red) are presented along with the difference of the contributions (blue). Note that the vertical scale is the same in all spectra, allowing for a direct comparison of the different contributions.

electrons [32]. In addition, the neutralization process by recombination further decreases the final kinetic energies that can be acquired by these fragments. Altogether, we therefore expect the neutral atoms formed by recombination to have lower kinetic energies. The relative importance of the different contributions cannot be derived from the experiment, and a complex modeling is beyond the scope of this paper. The experimental results reported here provide an important reference for theory to test different models of recombination in expanding clusters.

We further study recombination of doubly-charged ions after cluster ionization by intense NIR pulses. Figures 4(b) and (d) show kinetic energy distributions for Ar^{2+} and Xe^{2+} ions. Despite the lower ionization potential of Xe in comparison to Ar, the ratio of Ar^{2+}/Ar$^+$ ions with pump + probe pulses is 0.5, while the Xe^{2+}/Xe$^+$ ion ratio is only 0.24 in the energy range between 0 and 70 eV. Assuming that the initial formation of Xe^{2+} ions by the pump laser is at least as efficient as the formation of Ar^{2+} ions, the low Xe^{2+} ion signal can be attributed to a very efficient recombination in the cluster core. Similar results were obtained for Ar–Xe clusters ionized by intense XUV pulses [13]. Note that in addition to recombination, multiphoton excitation by the pump pulse and electron impact excitation can in principle lead to the formation of excited ions as well. However, the previous results in singly-charged ions from NIR and XUV ionization of clusters indicate that recombination to excited states is the dominant process here as well. The comparably low Xe^{2+} ion signal with pump+probe pulses suggests that only a fraction of the overall electron-ion recombination is probed. We note that in the experiment only electron-ion recombination processes leading to the formation of excited atoms and ions are accessible, whereas recombination leading to the formation of ground state atoms and ions is not detected. In addition, only excited atoms with a sufficient reionization probability by the 790 nm probe pulse are recorded.

Above certain kinetic energies, the ion signal from the pump+probe experiment falls below the signal induced by the pump pulse only. This is e.g. visible in figure 4(c), where at kinetic energies above 25 eV the Ar$^+$ signal is reduced by the probe pulse. At the same time, an increase of the Ar^{2+} signal is observed in this kinetic energy range (figure 4(d)). The effect is attributed to the reionization of excited Ar$^+$ ions, which are then recorded as ions with charge states of 2 or higher. For Ar^{2+} ions a similar effect is observed, where for energies above 70 eV the probe pulse leads to a reduction of the Ar^{2+} ion yield (figure 4(d)). Note that ions with kinetic energies higher than shown in figure 4 cannot be measured with our detector, which can influence the reconstruction of the 3D momentum map by the Abel inversion algorithm. However, the main interest here lies

on the qualitative effects induced by the probe pulse predominantly leading to the generation of ions with kinetic energies in the range of our detector. Moreover, we have confirmed that the effects induced by the NIR pulses are as well observed in the original momentum distributions. This experiment shows that not only neutral excited atoms are formed inside the nanoplasma, but also a large fraction of singly- and doubly-charged excited ions.

5. Summary

In summary, we have investigated electron-ion recombination processes in expanding clusters that are ionized by intense XUV or NIR pulses. By making use of REAR, we found an extensive formation of excited atoms in both cases, underlining the general significance of recombination processes in nanoplasmas. These nanoplasma dynamics taking place in later expansion stages exhibit a very similar behavior for XUV and NIR pulses, even though the initial ionization mechanisms are completely different. Furthermore, recombination takes place irrespective of the cluster composition and is also shown to affect larger cluster fragments. We have observed that recombination leading to the formation of excited atoms becomes more important for increasing cluster size when using intense XUV pulses. After NIR ionization of mixed Ar–Xe clusters, recombination was found to preferentially take place in the Xe core of the cluster, in agreement with previous investigations in the XUV regime. In addition, higher charge states in the Xe core are efficiently quenched. REAR is also used to rationalize the kinetic energies of excited atoms that are formed by NIR ionization atoms: these fragments acquire a substantial acceleration in the nanoplasma, suggesting that they live as ions before recombination producing a neutral atom takes place.

References

[1] Saalmann U, Siedschlag C and Rost J M 2006 *J. Phys. B: At. Mol. Opt. Phys.* **39** 39–77
[2] Fennel T, Meiwes-Broer K-H, Tiggesbäumker J, Reinhard P-G, Dinh P M and Suraud E 2010 *Rev. Mod. Phys.* **82** 1793–842
[3] Lezius M, Dobosz S, Normand D and Schmidt M 1997 *J. Phys. B: At. Mol. Opt. Phys.* **30** 251
[4] Bostedt C *et al* 2008 *Phys. Rev. Lett.* **100** 133401
[5] Arbeiter M and Fennel T 2010 *Phys. Rev.* A **82** 013201
[6] Iwayama H *et al* 2010 *J. Phys. B: At. Mol. Opt. Phys.* **43** 161001
[7] Schütte B, Arbeiter M, Fennel T, Vrakking M J J and Rouzée A 2014 *Phys. Rev. Lett.* **112** 073003
[8] Shao Y L, Ditmire T, Tisch J W G, Springate E, Marangos J P and Hutchinson M H R 1996 *Phys. Rev. Lett.* **77** 3343–6
[9] Laarmann T *et al* 2005 *Phys. Rev. Lett.* **95** 063402
[10] Bostedt C *et al* 2010 *New J. Phys.* **12** 083004
[11] Jungreuthmayer C, Ramunno L, Zanghellini J and Brabec T 2005 *J. Phys. B: At. Mol. Opt. Phys.* **38** 3029
[12] Fennel T, Ramunno L and Brabec T 2007 *Phys. Rev. Lett.* **99** 233401
[13] Hoener M, Bostedt C, Thomas H, Landt L, Eremina E, Wabnitz H, Laarmann T, Treusch R, de Castro A R B and Moeller T 2008 *J. Phys. B: At. Mol. Opt. Phys.* **41** 181001
[14] Iwayama H, Nagasono M, Harries J R and Shigemasa E 2012 *Opt. Express* **20** 23174
[15] Krikunova M *et al* 2012 *J. Phys. B: At. Mol. Opt. Phys.* **45** 105101
[16] Arbeiter M, Peltz C and Fennel T 2014 *Phys. Rev.* A **89** 043428
[17] Schütte B, Campi F, Arbeiter M, Fennel T, Vrakking M J J and Rouzée A 2014 *Phys. Rev. Lett.* **112** 253401
[18] Gademann G, Ple F, Paul P-M and Vrakking M J J 2011 *Opt. Express* **19** 24922–32
[19] Frühling U *et al* 2009 *Nat. Photonics* **3** 523
[20] Schütte B, Frühling U, Wieland M, Azima A and Drescher M 2011 *Opt. Express* **19** 18833
[21] Hagena O F 1981 *Surf. Sci.* **106** 101
[22] Tchaplyguine M, Lundwall M, Gisselbrecht M, Ohrwall G, Feifel R, Sorensen S, Svensson S, Martensson N and Bjorneholm O 2004 *Phys. Rev.* A **69** 031201(R)
[23] Danylchenko O G, Doronin Y S, Kovalenko S I and Samovarov V N 2006 *JETP Lett.* **84** 324
[24] Eppink A T J B and Parker D H 1997 *Rev. Sci. Instrum.* **68** 3477–84
[25] Vrakking M J J 2001 *Rev. Sci. Instrum.* **72** 4084–9
[26] Schroedter L *et al* 2014 *Phys. Rev. Lett.* **112** 183401
[27] Zweiback J, Ditmire T and Perry M D 1999 *Phys. Rev.* A **59** R3166
[28] Siedschlag C and Rost J M 2005 *Phys. Rev.* A **71** 031401(R)
[29] Arbeiter M and Fennel Th 2011 *New J. Phys.* **13** 053022
[30] Chan W F, Cooper G, Guo X, Burton G R and Brion C E 1992 *Phys. Rev.* A **46** 149
[31] Rajeev R, Madhu Trivikram T, Rishad K P M, Narayanan V, Krishnakumar E and Krishnamurthy M 2013 *Nat. Phys.* B **9** 185–90
[32] Ditmire T, Donnelly T, Rubenchik A M, Falcone R W and Perry M D 1996 *Phys. Rev.* A **53** 3379